HHS Public Access

Author manuscript

J Am Coll Cardiol. Author manuscript; available in PMC 2015 May 12.

Published in final edited form as:

J Am Coll Cardiol. 2014 April 29; 63(16): 1657–1666. doi:10.1016/j.jacc.2014.02.533.

Impact of Mechanical Activation, Scar, and Electrical Timing on Cardiac Resynchronization Therapy Response and Clinical Outcomes

Kenneth C. Bilchick, MD, MS[1], **Sujith Kuruvilla, MD**[1], **Yasmin S. Hamirani, MD**[1], **Raghav Ramachandran, MS**[2], **Samantha A. Clarke, BS**[2], **Katherine M. Parker, PhD**[2], **George J. Stukenborg, PhD, MA**[4], **Pamela Mason, MD**[1], **John D. Ferguson, MBChB, MD**[1], **J. Randall Moorman, MD**[1], **Rohit Malhotra, MD**[1], **J. Michael Mangrum, MD**[1], **Andrew E. Darby, MD**[1], **John DiMarco, MD, PhD**[1], **Jeffrey W. Holmes, MD, PhD**[1,2], **Michael Salerno, MD, PhD**[1,2,3], **Christopher M. Kramer, MD**[1,3], and **Frederick H. Epstein, PhD**[2,3]

[1]Department of Medicine, Cardiovascular Division, University of Virginia Health System, Charlottesville, VA

[2]Department of Biomedical Engineering, University of Virginia Health System, Charlottesville, VA

[3]Department of Radiology and Medical Imaging, University of Virginia Health System, Charlottesville, VA

[4]Department of Public Health Sciences, University of Virginia Health System, Charlottesville, VA

Abstract

Objectives—Using cardiac magnetic resonance (CMR), we sought to evaluate the relative influences of mechanical, electrical, and scar properties at the left ventricular (LV) lead position (LVLP) on CRT response and clinical events.

Address for Correspondence: Kenneth C. Bilchick, M.D., M.S., F.A.C.C., F.H.R.S., University of Virginia Health System, Department of Medicine, Cardiology/Electrophysiology, P.O. Box 800158, Charlottesville, Virginia 22908, Phone: 434-924-2465; Fax: 815-346-5805; bilchick@virginia.edu.

Disclosures:

Dr. Bilchick has received support from the National Institutes of Health (NIH) (K23 grant HL094761); and has served as a consultant to Biosense Webster. Dr. Parker is an employee of Sorin Group USA, Inc. Dr. Mason has received grant support from Medtronic and Boston Scientific; and has received support from St. Jude Medical and Johnson & Johnson. Dr. Ferguson has received consulting support from Biosense Webster and St. Jude Medical; and has received honoraria from Medtronic. Dr. Malhotra has received grant support from Medtronic and Boston Scientific. Dr. Mangrum has received grant and consulting support from St. Jude Medical; and has received research funding from St. Jude Medical, Hansen Medical, EndoSense, CardioFocus, and Boston Scientific. Dr. Darby has served as a consultant for Biosense Webster; has received speaking honoraria from Medtronic; and has received research support from Boston Scientific. Dr. DiMarco has received consulting support from Medtronic, St. Jude Medical, and Boston Scientific. Dr. Holmes has received support from the NIH (R01 grant HL085160). Dr. Kramer has received grant support from Siemens Healthcare; and has served as a consultant to Synarc and St. Jude Medical. Dr. Epstein has received support from the NIH (R01 grant EB001763); and has received grant support from Siemens Healthcare. All other authors have reported that they have no relationships relevant to the contents of this paper to disclose.

Background—CMR cine displacement encoding with stimulated echoes (DENSE) provides high quality strain for overall dyssynchrony (circumferential uniformity ratio estimate [CURE, 0–1]) and timing of onset of circumferential contraction at the LVLP. CMR DENSE, late gadolinium enhancement, and electrical timing together could improve upon other imaging modalities for evaluating the optimal LVLP.

Methods—Patients had complete CMR studies and echocardiography before CRT. CRT response was defined as a 15% reduction in LV end-systolic volume. Electrical activation was assessed as the time from QRS-onset-to-LVLP-electrogram (QLV). Patients were then followed for clinical events.

Results—In 75 patients, multivariable logistic modeling accurately identified the 40 (53%) of patients with CRT response (AUC=0.95 [p<0.0001]) based on CURE (OR 2.59/0.1 decrease), delayed circumferential contraction onset at LVLP (OR 6.55), absent LVLP scar (OR 14.9), and QLV (OR 1.31/10 ms increase). The 33% of patients with CURE<0.70, absence of LVLP scar, and delayed LVLP contraction onset had a 100% response rate, whereas those with CURE≥0.70 had a 0% CRT response rate and a 12-fold increased risk of death, and the remaining patients had a mixed response profile.

Conclusions—Mechanical, electrical, and scar properties at the LVLP together with CMR mechanical dyssynchrony are strongly associated with echocardiographic CRT response and clinical events after CRT. Modeling these findings holds promise for improving CRT outcomes.

Keywords

cardiac resynchronization therapy; cardiac magnetic resonance; heart failure; myocardial infarction; ventricular tachycardia

Introduction

Outcomes after cardiac resynchronization therapy (CRT) are influenced by a complex interaction between the myocardial substrate and the left ventricular lead position (LVLP). The myocardial substrate may be characterized both by the pattern of mechanical activation (1) and the distribution of scar (2). Recent echocardiographic methods such as 3-D echocardiography and speckle tracking (3, 4) offer the potential for better performance over previous methods, as do dyssynchrony assessments based on cardiac magnetic resonance (CMR) (5) and the circumferential uniformity ratio estimate (CURE) (6–8). Scar in the posterolateral LV, a common location for the LV lead, has been associated with CRT nonresponse (9), while late-activated sites based on electrical parameters (LV lead electrical delay and QRS to LV intrinsic activation interval [QLV]) (10, 11) or mechanical criteria (12, 13) appear to be better locations for LV leads.

CMR is the gold standard for assessment of myocardial scar. We have recently shown that CMR displacement encoding with stimulated echoes (DENSE) generates high-quality circumferential strain data (5, 8, 14–16) that can precisely describe the state of mechanical dyssynchrony using the CURE parameter (6), which does not require manual detection of regional time to peak strain (8). We now report the results of a cohort study of patients referred for CRT based on the hypothesis that favorable CMR findings (lower CURE from

CMR DENSE, no scar at the LVLP, and delayed onset of circumferential contraction at the LVLP) and late electrical activation at the LVLP are strongly associated with CRT response and clinical events during follow-up. The clinical significance is that CMR applied this way could improve on current criteria (17, 18) for patient selection and facilitate more effective implementation of CRT.

Methods

Cohort Selection

The study was approved by the Institutional Review Board for Human Subjects Research at the University of Virginia. Patients were required to have a clinical indication for CRT based on established guidelines (18) and a glomerular filtration rate of at least 45 cc/min/ $1.73m^2$ in order to receive gadolinium.

CMR Protocol

Prior to the CRT procedure, patients underwent a research CMR protocol including steady-state free precession imaging, cine DENSE imaging, and late gadolinium enhancement (LGE) on a 1.5T Avanto scanner (Siemens Healthcare, Erlangen, Germany) with a 4-channel phased-array chest radiofrequency coil. Cine DENSE imaging (previously validated by comparison with myocardial tagging in heart failure) (8) was performed in 4 short-axis and 3 long-axis planes with displacement encoding applied in two orthogonal in-plane directions for each plane with the following parameters (14, 15): interleaved spiral readout with 6 interleaves per image; repetition time (TR)/echo time (TE) 17ms/1.9ms; slice thickness 8 mm; field of view 350 x 350 mm; flip angle 15°; pixel size 2.8 x 2.8 mm; fat suppression; and displacement-encoding frequency 0.1 cycles/mm.

Determination of Echocardiographic Volumes Before and After CRT

Standard 2D echocardiographic images with Doppler were obtained for all patients at baseline, then 3 months and 6 months after CRT with standard short- and long-axis views. The LV end-systolic volume (LVESV), end-diastolic volume (LVEDV), and ejection fraction (LVEF) before and after CRT were determined using Simpson's rule for 2-chamber and 4-chamber long axis views using GE EchoPAC software.

Clinical CRT Procedure

Patients then underwent the clinical CRT procedure. During the procedure, venograms of the coronary sinus were recorded in two projections. Final cine images of the leads were recorded in the usual left anterior oblique, anterior-posterior, and right anterior oblique projections.

Clinical Follow-up and Determination of CRT Response

The echo evaluation at 3 months included standard A-V and V-V optimization. CRT response was defined as a 15% reduction in LVESV at 6 months (or the last follow-up echo prior to death if the patient died prior to 6 months after implantation). After the procedure, subsequent clinic notes, device interrogations, and discharge summaries for inpatient

hospitalizations were reviewed for all study patients. Sustained ventricular tachyarrhythmia (VT) events were defined as episodes of ventricular tachycardia or ventricular fibrillation requiring ICD therapies or untreated ventricular tachyarrhythmia episodes greater than 30 seconds detected by the ICD, and these events were also recorded in the database.

CMR DENSE Image Processing and Strain Analysis

Following image acquisition, segmentation of the left ventricular (LV) myocardium was performed semi-automatically for cine DENSE images (19), a phase-unwrapping algorithm was applied to LV myocardium pixels, and displacements were calculated (5). Lagrangian strain was computed from displacements in 24 short-axis segments in multiple slices and then projected in both the radial and circumferential (E_{CC}) directions relative to the LV center of mass. LV volumes, mass, and ejection fraction were calculated from cine steady-state free precession images using Argus software (Siemens, Erlangen, Germany).

Evaluation of CMR Dyssynchrony, Strain Onset at the LVLP, and Electrical Activation at the LVLP

Dyssynchrony was assessed from four short-axis cine DENSE slices at basal, midbasal, midapical, and apical levels (with additional weight given to basal and midbasal slices) using the circumferential uniformity ratio estimate (CURE), which is based on the Fourier transform (FT) of the spatial distribution of strain as previously described (6–8). Briefly, CURE makes use of the zero-order power and first-order power from the Fourier analysis of this function to index dyssynchrony on a scale between 0 (dyssynchrony) and 1 (synchrony) (6). The characteristics of the E_{CC} curve at the LV lead implantation site were then determined with respect to time to peak E_{CC} and onset of E_{CC} (onset of circumferential contraction), which was defined as the time from QRS detection by the scanner's gating software (when DENSE encoding pulse are applied) to the onset of a negative slope of the E_{CC} curve. Regarding electrical activation, the QLV was calculated as previously described as the time from QRS onset to the electrogram at the LVLP, with a value of at least 95 ms associated with greater rates of CRT response in the SmartDelay determined AV Optimization (SMART-AV) Trial (11).

Evaluation of Myocardial Scar from Late Gadolinium Enhancement and Lead Position Relative to Scar

The lead position relative to scar from CMR late gadolinium enhancement (LGE) was determined using the "o'clock" method in all patients (20). In a subset of these patients, results from this method were also confirmed using a quantitative algorithm we developed and validated for lead localization, as previously described (21). Regarding the latter, we pre-calibrated standard fluoroscopy suites by imaging a phantom at multiple camera positions, then reconstructed and registered 3D lead positions with pre-procedure CMR. With this method, the LVLP was identified as the point on the epicardial surface at which the distances between the lead position and each of the three landmarks (coronary sinus os, RV apex, anterolateral mitral annulus) in the CMR coordinate space were most similar to the equivalent distances in the fluoroscopic space. This algorithm was implemented in custom software written using Matlab (v7.14, The Mathworks, Natick, MA).

In patients with previous myocardial infarction, scar was manually segmented from short-axis LGE images using the segmentation software Segment described above. Late gadolinium enhanced (LGE) tissue (scar tissue) had a signal intensity at least 2 standard deviations above the mean signal intensity in remote areas. Scar transmurality was measured as a fraction of wall thickness calculated over the circumference with a 5 degree moving average window, using custom software implemented in Matlab. Scar distribution and transmurality were displayed on a Hammer projection map of the epicardial surface (22) along with the LVLP, as shown in Figures 1 and 2.

Statistical Analysis

Statistical analysis was performed using SAS 9.3 (SAS Institute, Cary, North Carolina). The Wilcoxon two-sample test (Mann Whitney U-test) was used for univariate comparisons between continuous variables, and the Fisher exact test was used for univariate comparisons between categorical variables (as in Table 1).

Based on the hypothesis that CRT response would be strongly associated with overall dyssynchrony with CURE (continuous), mechanical stretch (delayed E_{CC} onset) at the LVLP (categorical), scar at the LVLP (categorical), and late electrical activation at the LVLP (continuous), bivariable logistic regression was used to estimate the probability of a 15% reduction in LVESV associated with these variables. Based on prior associations between scar burden and CRT outcomes (2), LV percent scar volume (continuous) was also analyzed using bivariable logistic regression, as was the LV mass index (continuous) parameter (based on a proposed mechanistic association between LV mass and CRT outcomes). Receiver operating characteristic (ROC) analysis was also performed, and the statistical significance of the area under the curve (AUC) was determined based on comparison with chance. Multivariable logistic regression was then performed based on this hypothesis-driven model with CURE, mechanical stretch at the LVLP (delayed E_{CC} onset), scar at the LVLP, and late electrical activation at the LVLP. Multivariable linear regression was then performed to estimate the percent change in LVESV as a variable function of these same four selected covariates from the multivariable logistic regression model.

Overfitting was evaluated based on the heuristic shrinkage estimator of van Houwelingen and Cessie, which should be ≥ 0.90 to rule out overfitting. For the multivariable logistic model, the shrinkage estimator was calculated as the (model likelihood chi square statistic – number of covariates)/(model likelihood chi square statistic). For the multivariable linear model, the shrinkage estimator was calculated as the ratio of the adjusted R^2 to the raw R^2 (23).

Kaplan Meier plots, the log-rank statistic, and Cox proportional hazards regression were used to analyze the associations for mechanical and scar findings with the clinical outcomes of death and sustained VT events (as defined above). For the clinical outcome of death, patients having favorable values for the CMR parameters in the multivariable logistic model (CURE < 0.70, no scar at the LVLP, and mechanical stretch at the LVLP) were compared with patients without this optimal CMR profile. The threshold value for CURE was based on a prior smaller study in a completely different cohort of patients (6).

Results

The cohort included 75 patients who had either a class I or class IIa indication for CRT according to current guidelines (18) and underwent implantation of a CRT defibrillator with subsequent clinical follow-up (median 2.6 years). The baseline characteristics are given in Table 1 for the entire cohort, as well as responders and nonresponders (LVESV improvement of at least 15%). With respect to LV structural characteristics based on CMR, the baseline LVEF (23.2% [IQR 15.0,28.4%]) was similar in responders and nonresponders, but the baseline LVESV index, baseline LVEDV index, stroke volume index, and baseline LVM index were all greater in nonresponders versus responders. The frequency of comorbid medical disease was also similar among responders and nonresponders.

With respect to events during follow up, 21.3% of patients died during a median follow-up of 2.6 years (IQR 1.6–3.8 years), while 16.0% had sustained ventricular tachycardia or fibrillation, and 26.7% were hospitalized with heart failure. As shown in Table 1, the rates of all these events were much higher for nonresponders compared with responders ($p < 0.009$–0.0001).

Based on echocardiography before and after CRT, favorable changes in LVESV, LVEDV, and LVEF were confirmed in responders but not in nonresponders. Although significant differences in LVESV are expected based on the definition of CRT response, results for all 3 parameters by group are reported for completeness. In responders, LVESV decreased (LVESV percent change −32.5% [IQR −49.5%,−22.2%]), and LVEF increased (absolute LVEF change of 16.5% [IQR 9%,23.5%]), while LVESV and LVEF failed to improve in nonresponders (LVESV percent change 3.3% [IQR −0.7%,22.1%], median LVEF absolute change −4% [IQR −8%,0%]) ($p<0.001$ for comparisons between responders and nonresponders). The LVEDV also decreased in responders (LVEDV percent change −12.9% [IQR −27.6%,−4.4%]) but remained about the same in nonresponders (LVEDV percent change 0.2% [IQR −3.7%,9.0%]) ($p<0.001$ for comparisons between responders and nonresponders).

As shown in Figures 1 and 2, mechanical and scar characteristics of the LV as a whole and at the LVLP were characterized in detail with cine DENSE and LGE. Figure 1 shows 3 examples of CRT responders, while Figure 2 shows 3 examples of CRT nonresponders. Consistent with our hypothesis, the comparison of nonresponders and responders showed significant differences not only in overall mechanical dyssynchrony with CURE but also in mechanical activation, electrical activation, and scar at the LVLP.

Bivariable logistic regression results for the four parameters hypothesized to have strong associations with CRT response (as well as the additional two variables of interest) are shown in Table 2. The corresponding multivariable model with these four parameters identified in our hypothesis is shown in Table 3. This model had an AUC=0.95 ($p < 0.0001$) without evidence of overfitting (shrinkage estimator=0.931) (Figure 3). The four covariates and corresponding odds ratios were: CURE for overall dyssynchrony (OR 2.59 per 0.1 decrease in CURE, 95% C.I. [1.58,4.23], absence of scar at the LVLP (OR=14.9 [2.56,86.6]), delayed onset of E_{CC} at the LVLP (OR=6.55 [1.18,36.4]), and delayed

electrical timing at the LVLP based on the QLV (OR 1.31 [1.04,1.65] per 10 ms increase in QLV), which was determined as the time from the QRS onset to the intraprocedural electrogram at the LVLP. The Nagelkerke maximum rescaled R^2 for the model was 0.72.

As shown in Table 4, the original covariates shown in the multivariable logistic model in Table 3 were also strongly associated with the percent change in LVESV (R^2=0.53) in a multivariable linear model, again without overfitting (shrinkage estimator=0.948) (23), consistent with an association not only with the presence but also with the degree of LV functional improvement. As shown in Figure 4, the LVESV decreased by 23.4% (IQR 17.1%,44.9%) in the 52 patients with CURE < 0.70 but increased by 7.2% (IQR 2.9%, 24.7%) in 23 patients with CURE ≥ 0.70 (p < 0.0001) (panel A). Regarding mechanical characteristics at the LV lead site, in the 52 patients with significant dyssynchrony by CURE (less than 0.70), the 33 patients with delayed E_{CC} onset (mechanical stretch) at the LVLP had a median decrease in the LVESV of 27.4% (IQR 18.0%,51.9%) after CRT, compared with 18.2% (IQR 1.5%,31.7%) in the 19 patients without delayed E_{CC} onset at the LVLP (p=0.01) (panel B). Furthermore, in the 38 patients with CURE < 0.70 and no scar at the LVLP, all 25 patients with delayed E_{CC} onset at the LVLP had a CRT response with a decrease of 37.1% (IQR 22.1%,52.0%) in LVESV compared with a decrease of only 17.6% (IQR 2.5%,22.4%) in the remaining patients without delayed E_{CC} onset at the LVLP (p=0.002) (panel D).

The multivariable logistic model for CRT response with CMR parameters only (CURE, delayed onset of E_{CC} at the LVLP, absence of LVLP scar, LV mass index) also performed very well (p<0.05 for maximum likelihood estimates for all parameters) with an overall AUC of 0.94 (p<0.0001) and Nagelkerke R^2 = 0.72 (p<0.05) (Supplemental Table 1). In addition, the multivariable linear model for percent change in LVESV including these same CMR parameters (Supplemental Table 2) also demonstrated similar performance compared with the original model reported in Table 4. Regarding scar burden, the LV percent scar volume was not included in these models because it was no longer associated with CRT response after adjustment for the presence of scar at the LVLP.

In addition to the associations between CMR findings and echocardiographic CRT response, favorable CMR findings were also associated with better clinical outcomes, as shown in the Kaplan-Meier curves for overall survival (logrank p=0.006) and ventricular tachyarrhythmias (p=0.01) in Figures 5 and 6, respectively. Patients with CURE ≥ 0.70 had a 12-fold increased risk of death (median follow-up of 2.6 years) compared with the group with the favorable CMR findings of CURE < 0.70, absence of LVLP scar, and delayed onset of E_{CC} at the LVLP (HR 11.9 [1.5–93.5]) (Figure 5). In addition, patients with CURE ≥ 0.60 had an increased risk of sustained ventricular tachyarrhythmias after CRT (HR 8.24 [1.06–63.9]) compared with patients with CURE < 0.60 (Figure 6).

Discussion

The principal finding of this study was that both echocardiographic CRT response and clinical outcomes such as death and sustained ventricular tachyarrhythmia after CRT can be explained with an integrated model based on mechanical and scar-related characterization of

the substrate for resynchronization from the pre-procedure CMR, with some additional discrimination provided by intraprocedural characterization of electrical timing at the LVLP. In addition, using models based on logistic, linear, and Cox proportional hazards regression, we have shown strong associations between pre-procedure imaging findings and both echocardiographic CRT response and clinical events. For example, the third of the patients with a favorable CMR profile (CURE < 0.70, delayed onset of E_{CC} at the LVLP, and absence of scar at the LVLP) enjoyed a 12-fold higher survival rate than the group of patients with CURE ≥ 0.70. In addition, none of the patients with CURE ≥ 0.70 had a CRT response (100% negative predictive value). The remaining patients had intermediate outcomes. In this way, this analysis has identified three distinct groups of patients expected to have a 0% CRT response and decreased survival after CRT, 100% CRT response and improved survival after CRT, or intermediate outcomes. With respect to other clinical events, increased ventricular tachyarrhythmia events in patients with higher CURE may have occurred because these patients did not have the beneficial antiarrhythmic effect of LV functional improvement to outweigh the potentially proarrhythmic effects of LV epicardial pacing (24).

The association between delayed onset of E_{CC} at the LVLP and CRT response was likely due to resynchronization of the most dysfunctional LV myocardium, allowing that tissue to contribute much more effectively to overall pump function. Furthermore, the use of time to strain onset rather than time to peak strain at the LVLP may be beneficial considering that the corresponding assessments of electrical timing are also measured during early systole rather than near the end of systole where late strain peaks occur. The independent contributions from regional mechanical and electrical activation are noteworthy. Furthermore, the finding that scar at the LVLP was associated with CRT nonresponse is distinguished from prior reports (9, 25) by the strength of association between LVLP scar and CRT response even after adjustment for overall dyssynchrony and other mechanical and electrical characteristics at the LVLP, which was determined using quantitative methods.

Lastly, the success of our models may be attributed to some extent to the high quality strain data that was obtained with CMR cine DENSE, as demonstrated in previous studies (5, 8, 15). In addition, use of the CURE parameter is advantageous because it does not introduce potential errors in the manual detection of regional time to peak strain, as seen with other dyssynchrony parameters, as we have shown previously (8). Of note, other echocardiographic modalities such as 3-D echo offer high quality E_{CC} data, and we have demonstrated that CURE can be effectively determined from 3-D echo (26), such that its use is not limited to CMR. From a more general perspective, these results have high clinical significance for improving patient selection and outcomes after CRT, with potential associated cost savings.

Limitations

We did not prospectively test the effect of altering the lead position based on CMR findings. Additional factors could have been analyzed, but the purpose of the study was to develop a parsimonious model including key factors related to scar, mechanical activation, and electrical timing. Regarding follow-up, although the primary outcomes measure was

reduction in LVESV at 6 months, there was significant variation in the follow-up durations for clinical outcomes such as overall survival that was addressed with censoring where appropriate in the survival analysis. Regarding the study cohort, patients were enrolled at a single institution, such that there may be differences between patients at this institution and other institutions receiving CRT. In addition, while this patient cohort provides strong evidence for this model, a large prospective multicenter trial would be appropriate prior to widespread clinical use.

Conclusions

Mechanical, electrical, and scar properties at the LVLP together with CMR mechanical dyssynchrony are strongly associated with echocardiographic CRT response and clinical events after CRT. Modeling these findings in patients referred for CRT holds promise for improving outcomes after the procedure.

Supplementary Material

Refer to Web version on PubMed Central for supplementary material.

Acknowledgments

We wish to acknowledge the contributions of clinical research coordinators Aly Blake and Irene Harvey, echocardiography technologists Kim Chadwell and Dale Fowler, and CMR technologist John Christopher.

Abbreviations

CMR	Cardiac Magnetic Resonance
CRT	Cardiac Resynchronization Therapy
CURE	Circumferential Uniformity Ratio Estimate
DENSE	Displacement Encoding with Stimulated Echoes
ECC	Circumferential Strain
LGE	Late Gadolinium Enhancement
LVEDV	Left Ventricular End Diastolic Volume
LVESV	Left Ventricular End Systolic Volume
LVLP	Left Ventricular Lead Position
LVM	Left Ventricular Mass
QLV	QRS to LV Electrogram Interval
VT	Ventricular Tachyarrhythmia

References

1. Bilchick KC, Helm RH, Kass DA. Physiology of biventricular pacing. Curr Cardiol Rep. 2007; 9:358–65. [PubMed: 17877930]

2. White JA, Yee R, Yuan X, et al. Delayed enhancement magnetic resonance imaging predicts response to cardiac resynchronization therapy in patients with intraventricular dyssynchrony. J Am Coll Cardiol. 2006; 48:1953–60. [PubMed: 17112984]

3. Gorcsan J III, Tanabe M, Bleeker GB, et al. Combined longitudinal and radial dyssynchrony predicts ventricular response after resynchronization therapy. J Am Coll Cardiol. 2007; 50:1476–83. [PubMed: 17919568]

4. Tanaka H, Nesser HJ, Buck T, et al. Dyssynchrony by speckle-tracking echocardiography and response to cardiac resynchronization therapy: results of the Speckle Tracking and Resynchronization (STAR) study. Eur Heart J. 2010; 31:1690–700. [PubMed: 20530502]

5. Spottiswoode BS, Zhong X, Hess AT, et al. Tracking myocardial motion from cine DENSE images using spatiotemporal phase unwrapping and temporal fitting. IEEE Trans Med Imaging. 2007; 26:15–30. [PubMed: 17243581]

6. Bilchick KC, Dimaano V, Wu KC, et al. Cardiac magnetic resonance assessment of dyssynchrony and myocardial scar predicts function class improvement following cardiac resynchronization therapy. JACC Cardiovasc Imaging. 2008; 1:561–8. [PubMed: 19356481]

7. Leclercq C, Faris O, Tunin R, et al. Systolic improvement and mechanical resynchronization does not require electrical synchrony in the dilated failing heart with left bundle-branch block. Circulation. 2002; 106:1760–3. [PubMed: 12356626]

8. Budge LP, Helms AS, Salerno M, Kramer CM, Epstein FH, Bilchick KC. MR Cine DENSE Dyssynchrony Parameters for the Evaluation of Heart Failure: Comparison With Myocardial Tissue Tagging. JACC Cardiovasc Imaging. 2012; 5:789–97. [PubMed: 22897992]

9. Bleeker GB, Kaandorp TA, Lamb HJ, et al. Effect of posterolateral scar tissue on clinical and echocardiographic improvement after cardiac resynchronization therapy. Circulation. 2006; 113:969–76. [PubMed: 16476852]

10. Singh JP, Fan D, Heist EK, et al. Left ventricular lead electrical delay predicts response to cardiac resynchronization therapy. Heart Rhythm. 2006; 3:1285–92. [PubMed: 17074633]

11. Gold MR, Birgersdotter-Green U, Singh JP, et al. The relationship between ventricular electrical delay and left ventricular remodelling with cardiac resynchronization therapy. Eur Heart J. 2011; 32:2516–24. [PubMed: 21875862]

12. Saba S, Marek J, Schwartzman D, et al. Echocardiography-guided left ventricular lead placement for cardiac resynchronization therapy: results of the Speckle Tracking Assisted Resynchronization Therapy for Electrode Region trial. Circ Heart Fail. 2013; 6:427–34. [PubMed: 23476053]

13. Khan FZ, Virdee MS, Palmer CR, et al. Targeted left ventricular lead placement to guide cardiac resynchronization therapy: the TARGET study: a randomized, controlled trial. J Am Coll Cardiol. 2012; 59:1509–18. [PubMed: 22405632]

14. Kim D, Gilson WD, Kramer CM, Epstein FH. Myocardial tissue tracking with two-dimensional cine displacement-encoded MR imaging: development and initial evaluation. Radiology. 2004; 230:862–71. [PubMed: 14739307]

15. Zhong X, Spottiswoode BS, Meyer CH, Kramer CM, Epstein FH. Imaging three-dimensional myocardial mechanics using navigator-gated volumetric spiral cine DENSE MRI. Magn Reson Med. 2010; 64:1089–97. [PubMed: 20574967]

16. Ernande L, Thibault H, Bergerot C, et al. Systolic myocardial dysfunction in patients with type 2 diabetes mellitus: identification at MR imaging with cine displacement encoding with stimulated echoes. Radiology. 2012; 265:402–9. [PubMed: 22929334]

17. Bryant AR, Wilton SB, Lai MP, Exner DV. Association between QRS duration and outcome with cardiac resynchronization therapy: a systematic review and meta-analysis. J Electrocardiol. 2013; 46:147–55. [PubMed: 23394690]

18. Tracy CM, Epstein AE, Darbar D, et al. 2012 ACCF/AHA/HRS focused update of the 2008 guidelines for device-based therapy of cardiac rhythm abnormalities: a report of the American College of Cardiology Foundation/American Heart Association Task Force on Practice Guidelines. J Am Coll Cardiol. 2012; 60:1297–313. [PubMed: 22975230]

19. Spottiswoode BS, Zhong X, Lorenz CH, Mayosi BM, Meintjes EM, Epstein FH. Motion-guided segmentation for cine DENSE MRI. Med Image Anal. 2009; 13:105–15. [PubMed: 18706851]

20. Albertsen AE, Nielsen JC, Pedersen AK, Hansen PS, Jensen HK, Mortensen PT. Left ventricular lead performance in cardiac resynchronization therapy: impact of lead localization and complications. Pacing Clin Electrophysiol. 2005; 28:483–8. [PubMed: 15955178]

21. Parker KM, Bunting E, Malhotra R, et al. Post-Procedure Mapping of Cardiac Resynchronization Lead Position Using Standard Fluoroscopy Systems: Implications for the Nonresponder with Scar. Pacing Clin Electrophysiol. 2014; 37:757–67. [PubMed: 24472061]

22. Herz SL, Ingrassia CM, Homma S, Costa KD, Holmes JW. Parameterization of left ventricular wall motion for detection of regional ischemia. Ann Biomed Eng. 2005; 33:912–9. [PubMed: 16060531]

23. Harrell FE Jr, Lee KL, Mark DB. Multivariable prognostic models: issues in developing models, evaluating assumptions and adequacy, and measuring and reducing errors. Stat Med. 1996; 15:361–87. [PubMed: 8668867]

24. Medina-Ravell VA, Lankipalli RS, Yan GX, et al. Effect of epicardial or biventricular pacing to prolong QT interval and increase transmural dispersion of repolarization: does resynchronization therapy pose a risk for patients predisposed to long QT or torsade de pointes? Circulation. 2003; 107:740–6. [PubMed: 12578878]

25. Ypenburg C, van Bommel RJ, Delgado V, et al. Optimal left ventricular lead position predicts reverse remodeling and survival after cardiac resynchronization therapy. J Am Coll Cardiol. 2008; 52:1402–9. [PubMed: 18940531]

26. Driver K, Ramachandran R, Kuruvilla S, et al. Relationship Between Reverse Remodeling and Resolution of Mechanical Dyssynchrony After Cardiac Resynchronization Therapy: Comparison of Strain Imaging With 3-D Echocardiography, Cardiac Magnetic Resonance, and Speckle Tracking Echocardiography (abstr). Circulation. 2013; 128:A17665.

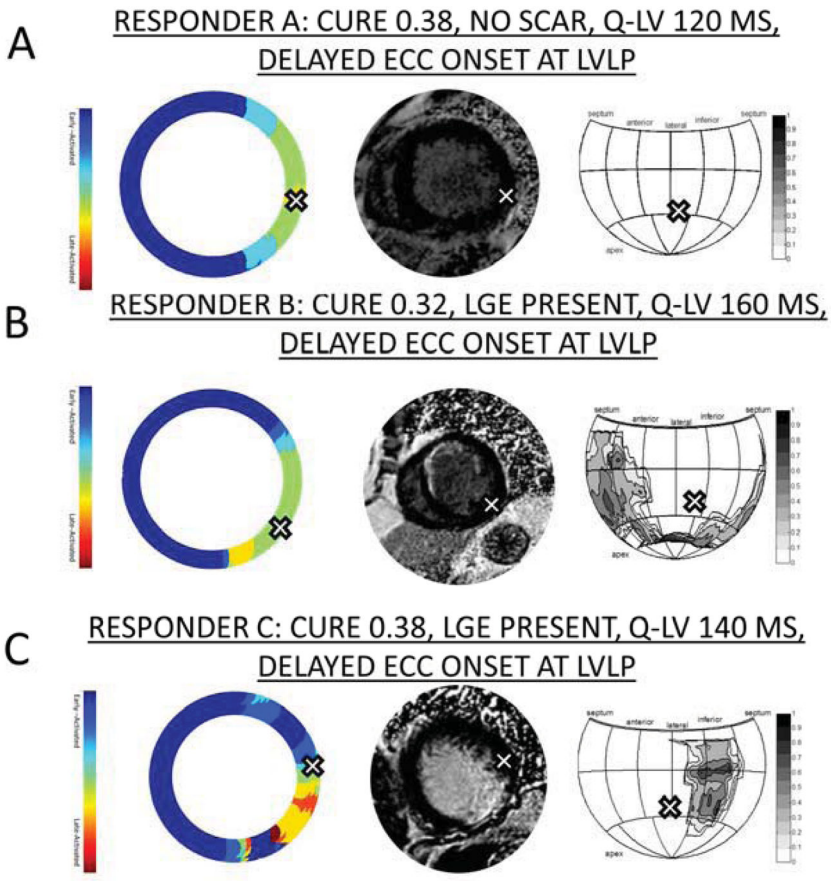

Figure 1. Scar and Time to E_{CC} Onset for Three CRT Responders

-- A) Patient with dyssynchrony, no scar, and delayed E_{CC} onset at the LVLP. B) Patient with dyssynchrony, anteroseptal infarct, and delayed E_{CC} onset at the LVLP. C) Patient with dyssynchrony, posterolateral infarct, and LVLP in an anterolateral segment with delayed E_{CC} onset and no scar.

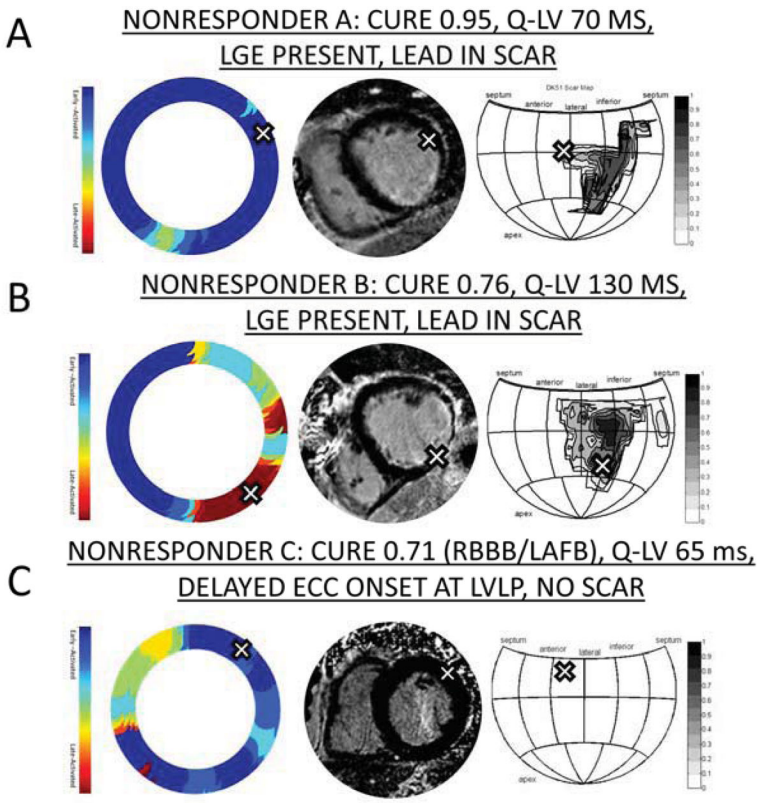

Figure 2. Scar and Time to E_{CC} Onset for Three CRT Nonresponders

-- A) Patient with minimal dyssynchrony and LVLP in anterolateral segment with scar. B) Patient with borderline dyssynchrony associated with posterolateral infarct and LVLP in scar. C) Patient with RBBB/left anterior fascicular block (LAFB) with QRS duration 180 ms, borderline dyssynchrony, no scar, and LVLP in early-activated segment. The late anteroseptal activation is associated with bifascicular block.

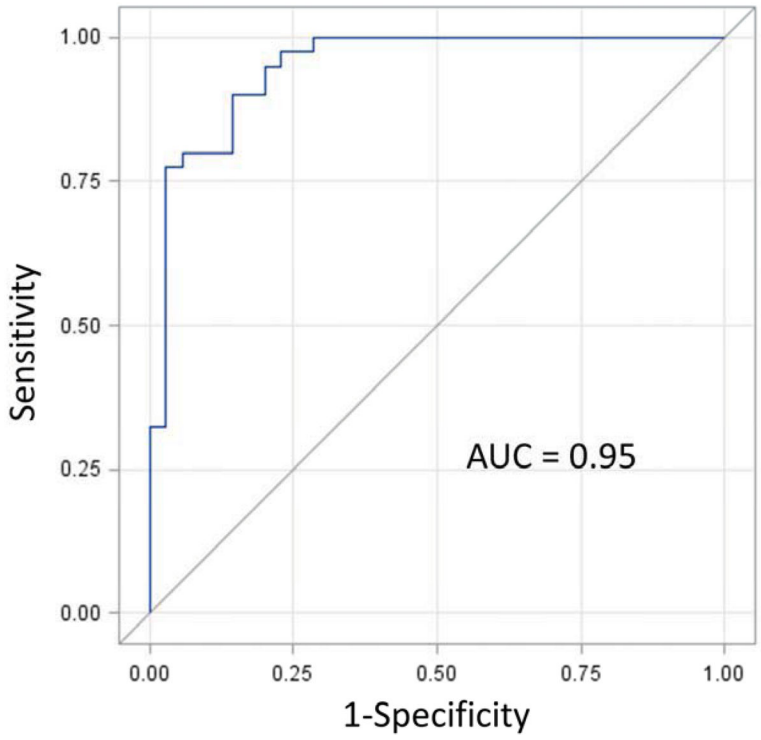

Figure 3. ROC Analysis for the Multivariable Logistic Model

-- The receiver operating characteristic (ROC) curve is shown for the multivariable logistic model in Table 3, as described in the text.

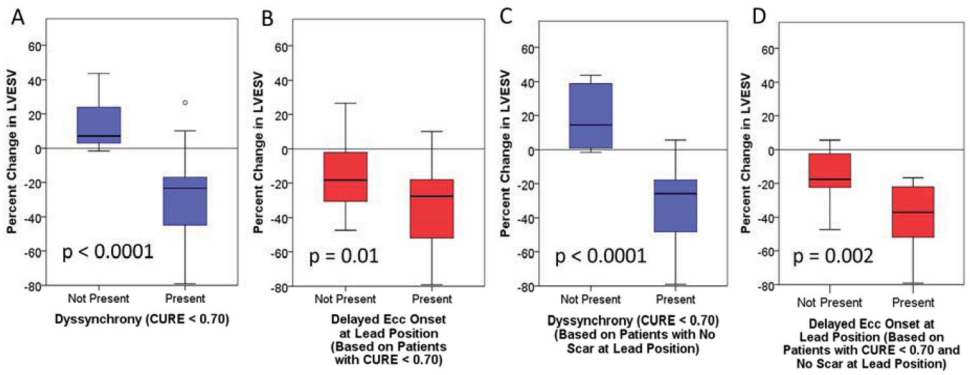

Figure 4. Box Plots for CRT Response in Selected

Subgroups -- A) Greater CRT response is present with CURE < 0.70. B) Greater CRT response is present with delayed E_{CC} onset at the LVLP among patients with CURE < 0.70. C) Differences in CRT response with CURE < 0.70 (as shown in panel A) including only patients without LVLP scar. D) Compared with panel B, patients without scar at the LVLP and CURE < 0.70 have even more pronounced differences in CRT response based on the presence or absence of delayed E_{CC} onset.

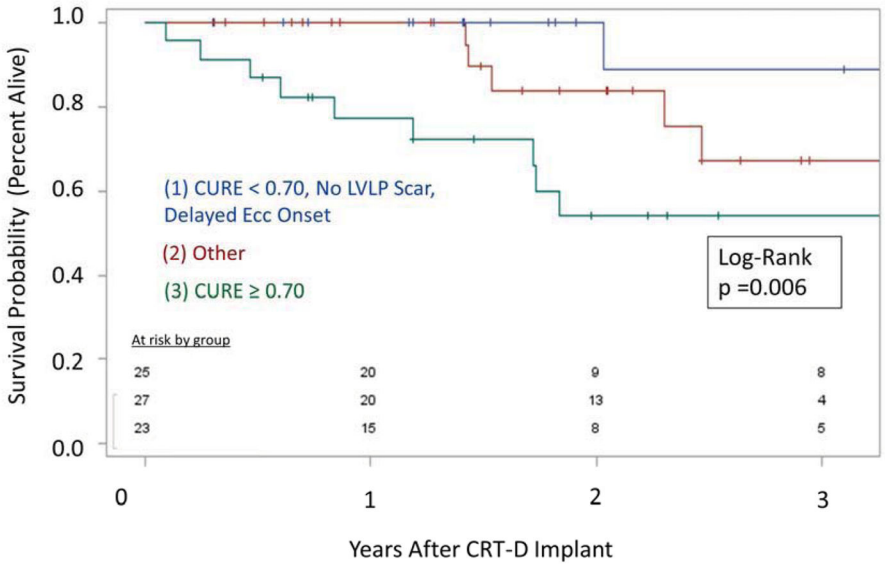

Figure 5. Survival Based on Favorable and Unfavorable CMR Baseline Profiles

-- Overall survival is markedly better for the 33% of patients (blue) with a favorable CMR profile (CURE < 0.70, no LVLP scar, delayed E_{CC} onset at LVLP) compared with the 31% of patients (red) without dyssynchrony by CURE (CURE ≥ 0.70). The remaining patients (green) had intermediate survival.

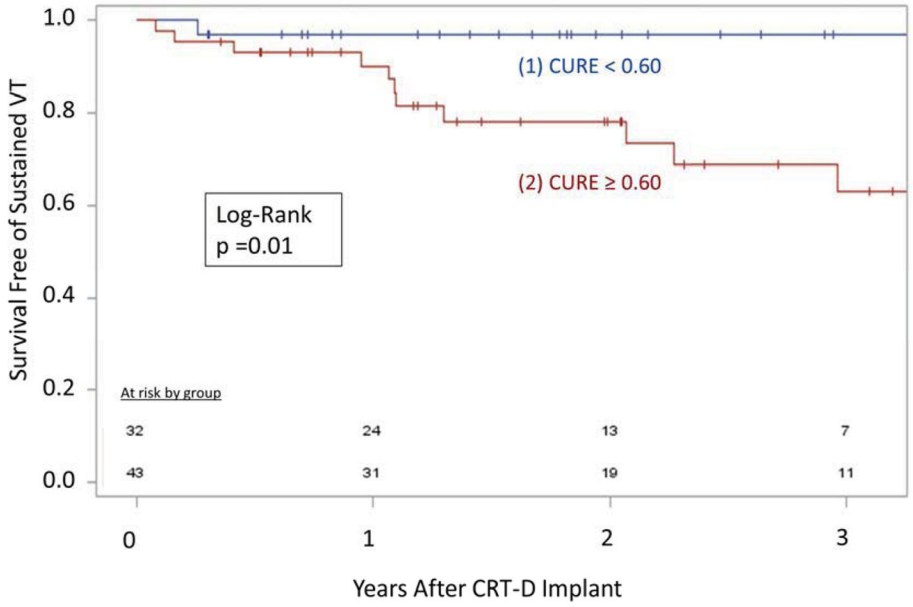

Figure 6. Ventricular Tachycardia and Dyssynchrony

-- Patients receiving CRT without prominent dyssynchrony (CURE ≥ 0.60) had increased ventricular tachyarrhythmias compared with patients with CURE < 0.60.

Table 1

Baseline Characteristics of CRT Responders and Nonresponders

	ALL (n=75)	RESPONDER (n=40)	NONRESPONDER (n=35)	p-value
Demographic/Clinical*				
Age, years	65.9 (57.8–74.3)	65.3 (57.7–72.6)	67.9 (59.2–76.4)	0.35
Female Gender	19 (25.3)	16 (40.0)	3 (8.6)	0.003
NYHA Class II/III/IV	3/71/1 (4.0/94.7/1.3)	3/37/0 (7.5/92.5/0)	0/34/1 (0/97.1/2.9)	0.17
CMR imaging parameters*				
LVEF, %	23.2 (15.0–28.4)	22.8 (16.1–27.9)	23.2 (13.8–28.4)	0.81
LVEDV index, ml	122 (104.1–151.0)	110.0 (91.4–139.3)	133.7 (110.5–155.6)	0.007
LVESV index, ml	96.9 (78.0–126.4)	88.0 (71.6–116.1)	109.3 (86.8–136.6)	0.02
SV index, ml	26.8 (21.2–33.9)	26.1 (21.0–28.0)	31.0 (24.0–38.0)	0.03
LV mass index, g/m^2	70.9 (59.4–82.9)	63.6 (49.5–80.7)	74.6 (66.0–90.2)	0.006
LGE present	41 (54.7)	17 (42.5)	24 (68.6)	0.04
LV per. scar volume (%)	4.3 (0–12.7)	0 (0–12.3)	7.3 (0–12.9)	0.12
CURE	0.61 (0.36–0.74)	0.37 (0.26–0.61)	0.75 (0.64–0.81)	<0.0001
Electrical activation and scar at LV lead*				
QLV	108 (72–140)	125 (107–143)	90 (60–105)	0.0002
Lead position in scar	28 (37.3)	8 (20.0)	20 (57.1)	0.002
Initial mechanical stretch	43 (57.3)	29 (72.5)	14 (40)	0.006
ECG parameters*				
QRS Duration, ms	155 (140–170)	160 (150–172)	150 (134–170)	0.12
LBBB	67 (89.3)	39 (97.5)	28 (80.0)	0.02
Comorbid conditions*				
Prior MI	34 (45.3)	14 (35.0)	20 (57.1)	0.06
Prior CABG	9 (12.0)	4 (10.0)	5 (14.3)	0.72
Chronic kidney disease	15 (20.0)	10 (25.0)	5 (14.3)	0.38
Diabetes mellitus	21 (28.0)	9 (22.5)	11 (34.3)	0.30
Peripheral art. disease	9 (12.0)	3 (7.5)	6 (17.1)	0.28
Hypertension	41 (54.7)	24 (60.0)	17 (48.6)	0.36
Prior stroke/TIA	7 (9.3)	5 (12.5)	2 (5.7)	0.43
Obstructive Sleep Apnea	15 (20.0)	7 (17.5)	8 (22.9)	0.58
Events during follow-up*				
Death	16 (21.3)	2 (5.0)	14 (40.0)	0.0004
Sustained VT	12 (16.0)	2 (5.0)	10 (28.6)	0.01
HF hospitalization	20 (26.7)	3 (7.5)	17 (48.6)	<0.0001

*Values are median (IQR) for continuous variables and number (%) for categorical variable.

The numbers in parentheses for NYHA class are the percentages of patients in each class.

Table 2

Bivariable Logistic Regression for CRT Response

Covariate	OR (95% CI)	Wald χ^2 (p-value)	AUC p-value	Sens./Spec.
MECHANICAL DYSSYNCHRONY				
CURE				
Continuous (0.1decrease)	2.20 (1.56–3.16)	19.66 (<0.0001)	0.87 (<0.0001)	--
Dichotomous (<0.70)*	--	--	0.82 (<0.0001)	100/65.7
LV LEAD POSITION				
Early Mechanical Stretch	3.95 (1.50–10.4)	7.73 (0.005)	0.66 (0.003)	72.5/60.0
Lead Not in Scar	5.33 (1.92–14.9)	10.27 (0.001)	0.69 (0.0005)	80.0/60.0
QLV				
Continuous (10ms)	1.31 (1.12–1.54)	11.67 (0.0006)	0.76 (<0.0001)	--
Dichotomous (≥95ms)	6.73 (2.26–20.1)	11.68 (0.0006)	0.70 (0.0001)	85.0/57.1
GLOBAL LV STRUCTURE				
LV Percent Scar Volume				
Continuous (per 10%)	0.79 (0.52–1.21)	1.18 (0.28)	0.59 (0.16)	--
Dichotomous (≤20%)	3.17 (0.574–17.5)	1.75 (0.19)	0.55 (0.18)	95.0/14.3
LV Mass Index				
Continuous (per 10 g/m^2)	0.75 (0.59–0.96)	5.44 (0.02)	0.68 (0.002)	
Dichotomous (≤70g/m^2)	2.29 (0.904–5.80)	3.05 (0.08)	0.60 (0.08)	53.3/62.9

* Likelihood ratio could not be calculated due to 0% responders with CURE ≥ 0.70

Table 3

Multivariable Logistic Regression Model for Echocardiographic CRT Response

Model Variable	OR (95% CI)	Wald χ^2	P-value <0.0001
CURE (per 0.1 decrease)	2.59 (1.58–4.23)	14.4	
Lead Position Not in Scar	14.9 (2.56–86.6)	9.03	0.003
Mechanical Stretch at LVLP*	6.55 (1.18–36.4)	4.61	0.03
QLV (per 10 ms increase)	1.31 (1.04–1.65)	5.36	0.02

Max rescaled R^2=0.72, AUC 0.95 (p<0.001

*Equivalent to Delayed E_{CC} Onset

Table 4

Multivariable Linear Regression Model for Percent Change in LVESV

Model Variable	Model Coefficient	Standard Error	P-value	Standardized Coefficient
Intercept	−0.201	0.115	0.08	0
CURE (0–1)	0.608	0.107	<0.0001	0.502
Lead Position Not in Scar	−0.1165	0.04727	0.02	−0.209
Mechanical Stretch at LVLP*	−0.094794	0.0483	0.054	−0.172
QLV (ms)	−0.00139	0.000679	0.05	−0.185

R^2 = 0.53; Adjusted R^2 = 0.50

*Equivalent to Delayed E_{CC} Onset